Heliyon 10 (2024) e29168

Contents lists available at ScienceDirect

Heliyon

journal homepage: www.cell.com/heliyon

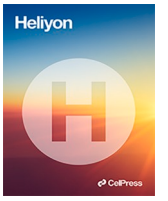

Research article

Oroxin A from *Oroxylum indicum* improves disordered lipid metabolism by inhibiting SREBPs in oleic acid-induced HepG2 cells and high-fat diet-fed non-insulin-resistant rats

Tianqi Cai [a], Xiaoxue Xu [a], Ling Dong [a], Shufei Liang [a], Meiling Xin [a], Tianqi Wang [b], Tianxing Li [c], Xudong Wang [d], Weilong Zheng [e], Chao Wang [a], Zhengbao Xu [a], Meng Wang [a], Xinhua Song [a], Lingru Li [c,***], Jingda Li [b,**], Wenlong Sun [a,*]

[a] *School of Life Sciences and Medicine, Shandong University of Technology, Zibo, Shandong, 255000, People's Republic of China*
[b] *College of Life Science, Yangtze University, Jingzhou, Hubei, 434000, People's Republic of China*
[c] *National Institute of TCM Constitution and Preventive Medicine, Beijing University of Chinese Medicine, Beijing, 100000, People's Republic of China*
[d] *College of Pharmaceutical Science, Zhejiang University of Technology, Hangzhou, Zhejiang 310000, People's Republic of China*
[e] *Institute of Biomass Resources, Taizhou University, Taizhou, Zhejiang, 317700, People's Republic of China*

ARTICLE INFO

Keywords:
Disordered lipid metabolism
Hyperlipidaemia
NAFLD
Oroxin A
SREBPs

ABSTRACT

Background: Lipid metabolism disorders have become a major global public health issue. Due to the complexity of these diseases, additional research and drugs are needed. Oroxin A, the major component of *Oroxylum indicum* (L.) Kurz (Bignoniaceae), can improve the lipid profiles of diabetic and insulin-resistant (IR) rats. Because insulin resistance is strongly correlated with lipid metabolism, improving insulin resistance may also constitute an effective strategy for improving lipid metabolism. Thus, additional research on the efficacy and mechanism of oroxin An under non-IR conditions is needed.

Methods: In this study, we established lipid metabolism disorder model rats by high-fat diet feeding and fatty HepG2 cell lines by treatment with oleic acid and evaluated the therapeutic effect and mechanism of oroxin A *in vitro* and *in vivo* through biochemical indicator analysis, pathological staining, immunoblotting, and immunofluorescence staining.

Results: Oroxin A improved disordered lipid metabolism under non-IR conditions, improved the plasma and hepatic lipid profiles, and enhanced the lipid-lowering action of atorvastatin. Additionally, oroxin A reduced the total triglyceride (TG) levels by inhibiting sterol regulatory element-binding protein 1 (SREBP1) expression and reducing the expression of acetyl coenzyme A carboxylase (ACC) and fatty acid synthase (FASN) *in vivo* and *in vitro*. Oroxin A also reduced the total cholesterol (TC) levels by inhibiting SREBP2 expression and reducing HMGCR expression *in vivo* and *in vitro*. In addition, oroxin A bound to low-density lipoprotein receptor (LDLR) and increased AMPK phosphorylation.

Conclusions: Our results suggested that oroxin A may modulate the nuclear transcriptional activity of SREBPs by binding to LDLR proteins and increasing AMPK phosphorylation. Oroxin A may thus

* Corresponding author. Institute of Biomedical Research, School of Life Sciences, Shandong University of Technology, Zibo, Shandong, 255000, People's Republic of China.
** Corresponding author.
*** Corresponding author.
E-mail addresses: lilingru912@163.com (L. Li), jingdali_shenqi@163.com (J. Li), 512649113@qq.com (W. Sun).

https://doi.org/10.1016/j.heliyon.2024.e29168
Received 3 August 2023; Received in revised form 30 March 2024; Accepted 2 April 2024
Available online 3 April 2024

reduce lipid synthesis and could be used for the treatment and prevention of lipid metabolism disorders.

1. Introduction

Lipid metabolism disorders, which mainly include hyperlipidaemia and nonalcoholic fatty liver disease (NAFLD), have become major global health security issues associated with changes in people's living standards and diet structure [1,2]. More than 20% of people suffer from these diseases worldwide. In addition, lipid metabolism disorders affect the development and progression of many other diseases, such as type 2 diabetes and atherosclerosis, and thus reduce the quality of life [3,4]. Therefore, an effective approach for hampering the development of lipid metabolism disorders is urgently needed. Currently, there are various drugs for treating lipid metabolism disorders, especially hyperlipidaemia. For example, statins are 3-hydroxy-3-methylglutaryl coenzyme A reductase inhibitors and are the most efficient drugs for the treatment of hyperlipidaemia. However, these drugs also have several disadvantages; in patients with severe disorders, the administration of high-dose statins does not increase the hypolipidaemic effects of these agents and can negatively affect human health by causing damage to kidney function, liver injury, and gastrointestinal dysfunction [5]. Additionally, statins do not effectively reduce hepatic fat accumulation, and no Food and Drug Administration (FDA)-approved drugs are available for the treatment of NAFLD [6]. Thus, further research on and drugs for lipid metabolism disorders are needed.

Natural products are important sources of many active ingredients in the drug discovery process and have the advantages of being naturally accessible, safe, and efficacious and having few side effects. When used in the prevention and treatment of various diseases, the bioactive components in natural products have a significant impact on the physiological activity of humans. The search for active ingredients from natural resources such as lead compounds is an effective strategy for developing new drugs. Recently, the positive effects of natural products on lipid metabolism disorders have attracted increasing attention. *Nie* et al. reviewed the application of natural bioactive components, including flavonoids, anthraquinones, saponins, alkaloids, proteins, and polysaccharides, for lipid metabolism disorders [7]. In addition, hesperidin and baicalein have been found to ameliorate lipid metabolism disorders by decreasing the hepatic and plasma lipid profiles in high-fat diet (HFD)-fed rats [8,9]. *O. indicum* is a traditional Chinese medicine that was first described in "Ben Cao Gang Mu Shi Yi", has been used clinically for several hundred years for respiratory and digestive system diseases [10]. Oroxin A, which is also known as baicalein-7-*O*-glucoside (PubChem CID: 5320313), is a flavonoid extracted from *O. indicum* seeds, accounts for nearly 30% of *O. indicum* seed extracts and exhibits antibacterial, antioxidant, antitumour, and other biological activities [11,12]. In addition, our previous research using mice showed that oroxin A can decrease the blood glucose levels, increase the sensitivity to insulin and improve lipid metabolism during the progression from prediabetes to diabetes, suggesting that oroxin A might exert a therapeutic effect on lipid metabolism disorders under conditions of insulin resistance [13,14]. These studies indicate that oroxin A, a natural active ingredient, is not only highly abundant in and easily obtained from *O. indicum* but also has the potential to be a lead compound for ameliorating lipid metabolism disorders, which indicates its high value for research and development. However, insulin resistance might induce lipid metabolism, and improving insulin resistance may be an effective strategy for improving lipid metabolism. Therefore, evaluating the effect of oroxin A on lipid metabolism disorders under non-insulin-resistant (IR) conditions is essential. To address this issue, the mechanism by which oroxin A improves lipid metabolism disorders could be explored under non-IR conditions. Furthermore, based on the lipid-lowering mechanism of oroxin A, identification of a strategy that combines statins and oroxin A to reduce the damage caused by high-dose statins is important.

In this study, we evaluated the role of oroxin A in disordered lipid metabolism and its potential mechanisms in HFD-fed non-IR rats and oleic acid-induced fatty HepG2 cells. Furthermore, we evaluated the synergistic effect of oroxin A and statins on hypolipidaemia.

2. Materials and methods

2.1. Materials

A protein assay kit, a protein extraction kit, a glucose assay kit (glucose oxidase method), and total cholesterol (TC), total triglyceride (TG), low-density lipoprotein cholesterol (LDLC), high-density lipoprotein cholesterol (HDLC), aspartate transaminase (AST), and alanine transaminase (ALT) kits were purchased from the Jiancheng Institute of Biotechnology (Nanjing, China). An insulin kit was purchased from Cusabio Technology Co., Ltd. (Wuhan, China). A Western Bright ECL kit, Dulbecco's modified Eagle's medium (DMEM), antibiotics, Lipofectamine 3000, foetal bovine serum, and trypsin were purchased from Solarbio Co., Ltd. (Beijing, China). Hygromycin B was purchased from Roche Co., Ltd. (Basel, Switzerland). Polyvinylidene fluoride (PVDF) membranes were purchased from Millipore Co., Ltd. (Massachusetts, USA). A luciferase assay kit and a luciferase reporter vector were purchased from Promega Co., Ltd. (Shanghai, China). HepG2 (human hepatocellular carcinoma) cells were obtained from American Type Culture Collection (Maryland, USA). HFD chow (D16492) containing 36.4% carbohydrates, 25.6% fat, 20% protein, 1% cholesterol and 0.1% bile acid was purchased from SYSE Co., Ltd. (Changzhou China). Recombinant mouse low-density lipoprotein receptor (LDLR) protein (ab206024) was purchased from Abcam (Cambridge, UK). Primary antibodies against precursor sterol regulatory element-binding protein 1 (pSREBP1; 1:1000, PA005992) and phospho-SREBP1 (1; 1000, PA050140) were purchased from Cusabio Technology Co., Ltd. (Wuhan, China). A primary antibody against precursor sterol regulatory element-binding protein 2 (pSREBP2; 1:1000, ab30682) was purchased from Abcam (Cambridge, UK), and a primary antibody against phospho-SREBP2 (Ser455) (pSREBP2; 1:1000, PA5-106042) was purchased from Thermo Fisher Scientific (Massachusetts, USA). Primary antibodies against acetyl coenzyme A

carboxylase (ACC; 1:1000; bs2745R), fatty acid synthase (FASN; 1:1000; bs1498R), 3-hydroxy-3-methylglutaryl CoA reductase (HMGCR; 1:100 bsm-52822R), and mature SREBP1 (mSREBP1; 1:1000; bs1402R) were purchased from Bioss Technology Co., Ltd. (Beijing, China). Primary antibodies against β-actin (1:1,000, K200058 M) and secondary antibodies were purchased from Solarbio Co., Ltd. Primary antibodies against sterol regulatory element-binding protein 2 (SREBP2) (1:1000, ab30682) and LDLR (ab30532) were purchased from Abcam (Cambridge, UK), and a primary antibody against phospho-SREBP2 (Ser455) (1:500, PA5-64716) was purchased from Thermo Fisher Scientific, Inc. (Massachusetts, USA).

2.2. Preparation of oroxin A

Oroxin A (purity higher than 96%; Fig. S1, Table S1, and Table S2) was isolated from *O. indicum* following previously described methods [13,15]. Briefly, *O. indicum* seed extract was dissolved in ethanol, applied to a reversed-phase column (ODS-C18) and eluted with 20–80% acetonitrile to obtain four fractions. Fraction 2 was concentrated and injected into the prepacked ODS column again to obtain pure oroxin A.

2.3. ELISA and docking experiments

2.3.1. Protein binding assay

Based on previous studies, we measured the binding efficiency of LDLR-oroxin A via an enzyme-linked immunosorbent assay (ELISA) [16]. A polystyrene plate was coated with oroxin A at a range of concentrations, incubated at 4 °C overnight and blocked with 1% gelatine for 2 h. After these steps, recombinant LDLR protein (50 μL/well, 20 μg/mL) was added, and the mixture was incubated for 1 h. The HRP-labelled goat anti-mouse IgG antibody was added for the detection of LDLR. Notably, the plate was washed three times with PBS after each step. After incubation with the secondary antibody, the samples were visualized. H_2O_2 and *o*-phenylenediamine were added for colour development, and the reaction was stopped by the addition of 2 mM sulfuric acid. Subsequently, the absorbance at 492 nm was measured within the specified time.

2.3.2. Docking experiment

Docking was carried out according to previous methods [13]. In brief, the ligand-binding domain structure of the LDLR protein was prepared according to a previously described method [13] and was derived from the Protein Data Bank (PDB ID: 3SO6, www.rcsb.org). The Schrodinger Maestro 9.4 package was subsequently used to predict the binding of the ligand-binding domain of the LDLR protein to oroxin A. In particular, we generated a docking grid (36 × 36 × 36 Å) and selected five optimal conformations according to the empirical Glide (G) scores (kcal/mol).

2.4. In vitro experiments

2.4.1. Cell culture

HepG2 cells were cultured in tissue culture flasks containing DMEM supplemented with 10% heat-inactivated foetal bovine serum (FBS) and antibiotics and incubated in 5% humidified CO_2 and 37 °C. The culture media was routinely changed every 2 days, and the cells were passaged by trypsinization before reaching confluence. The adipose HepG2 cell model was generated according to previously described methods with appropriate modifications [17]. Briefly, HepG2 cells were starved for 12 h and then treated with 1 mM oleic acid for 24 h to induce excessive fat accumulation; the differentiation of HepG2 cells was confirmed by assays of the TC and TG levels.

2.4.2. In vitro Oil Red O staining

HepG2 cells were inoculated in 10-cm culture dishes and cultured to 70%–80% confluence for the experiment. After starvation for 12 h, the HepG2 cells were treated with either DMSO or oroxin A (5 μM or 50 μM) in combination with 1 mM oleic acid and incubated for 24 h, whereas untreated cells served as the control cells. HepG2 cells were subsequently fixed with 1 ml of 2% formaldehyde and stained with Oil Red O according to previously described methods [8]. The stained samples were then observed at an appropriate magnification of 20×.

2.4.3. Assays of the cellular TC and TG levels

The cytotoxicity of oroxin A was determined in our previous study [13]. We determined whether the fatty HepG2 cell model was successfully established by measuring the cellular TC and TG levels. After successful model establishment, the cells in the treatment groups were treated with different concentrations (5 μM and 50 μM) of oroxin A, and the negative control cells were treated with DMSO. After treatment for 24 h, we determined the cellular TC and TG levels using commercial kits. Each treatment was repeated 3 times.

2.4.4. Assay of SREBP transcriptional activity

The transcriptional activity of SREBP in the cell model was assessed as previously described with a slight modification [9]. Briefly, three tandem SREBP-binding sites, 5′-AAAATCACCCCACTGCAAACTCCTCCCCCTGC-3′, were inserted into pGL4.26 by primer annealing to generate the SREBP reporter plasmid pSRE-Luc. HepG2 cells were cotransfected with pSRE-Luc and the control Renilla vector pRL-TK using Lipofectamine 3000. After 24 h, the cells were transfected into medium containing 200 μg/mL hygromycin B. The

medium was changed every three days until colonies formed. Individual colonies were visually identified and isolated using cloning cylinders. Furthermore, the cells were treated with different concentrations (0 μM, 5 μM, and 50 μM) of oroxin A and 1 mM oleic acid for 24 h, and the effect of oroxin A on the transcriptional activity of SREBP was then determined using a luciferase assay kit.

2.4.5. In vitro immunoblot analysis

After fatty HepG2 cells were treated with DMSO or oroxin A (5 μM or 50 μM) for 24 h (cell treatments with pAMPK, phospho-SREBP1, and phospho-SREBP2 were performed for 1 h, 1 h, and 6 h, respectively), we collected the cells and extracted proteins using a protein extraction kit according to the instructions. We then separated the protein samples by 12% SDS–polyacrylamide gel electrophoresis (PAGE) to measure the mature SREBP1 (mSREBP1), mature SREBP2 (mSREBP2), AMPK, pAMPK and β-actin levels. We separated pSREBP1, phospho-SREBP, pSREBP2, phospho-SREBP2, ACC, FASN and HMGCR by 8% SDS–PAGE. The separated protein samples were transferred to a PVDF membrane, which was subsequently blocked with 5% skim milk for 4 h at room temperature. The membrane was then incubated with primary antibody diluted with Tris-buffered saline containing Tween-20 and 2.5% skim milk at 4 °C overnight. The immune complex can be recognized by a secondary antibody coupled to horseradish peroxidase. After the proteins were incubated with the secondary antibody, peroxidase activity was assessed by exposing the protein bands using the ECL kit, and the protein bands were quantified using ImageJ software. All protein expression levels were normalized to that of β-actin. Each treatment was repeated 3 times.

2.4.6. AMPK phosphorylation inhibition assay

After fatty HepG2 cells were starved for 12 h, the cells were treated with DMSO or 10 μM compound C (dorsomorphin) for 1 h and then with DMSO or oroxin A. The cellular TC and TG levels and SREBP transcriptional activity were then determined using the methods described in sections 2.4.3 and 2.4.4, respectively.

2.4.7. In vitro immunofluorescence staining

An *in vitro* immunofluorescence staining experiment was performed according to a previously reported method with slight modifications [18]. The cells were treated with different concentrations (0 μM, 5 μM, or 50 μM) of oroxin A for 24 h and then used for immunofluorescence staining *in vitro*. The fixed HepG2 cells were cultured for 10 min with BSA/FBS to block nonspecific binding sites and then cultured with PBS (pH 7.4) containing 1% SREBP1 or SREBP2 antibody. The cells were then subjected to three 5-min washes with 1 ml of PBS/FBS to remove unbound antibodies. The fixed HepG2 cells were incubated with 1% fluorophore-conjugated secondary antibodies. After the secondary antibody was added, the fixed HepG2 cells were covered with culture dishes and cultured in the dark for 60 min at room temperature. The cells were then subjected to three 5-min washes with 1 ml of PBS/FBS to remove unbound antibodies. Finally, the nuclei were stained with 4′,6-diaminophenylindole (DAPI), and the cells were blocked with neutral gel to observe the fluorescent signal using an Olympus IX81 microscope. If SREBP1 or SREBP2 underwent nuclear translocation, a FITC fluorescence signal was observed in the DAPI-stained nuclei for the quantification of SREBP1 or SREBP2.

2.5. In vivo experiments

2.5.1. Animal experiments

Male Sprague–Dawley rats (180–220 g) were purchased from the Shandong Laboratory Animal Center (Jinan, China) (permission number SCXK 2014-0007). The current study protocol followed international ethical guidelines, and all animal handling procedures were performed in a standard laboratory and approved by the Institutional Animal Care and Use Committee of Shandong University of Technology (YLX20210801).

2.5.2. Experiment 1

Eight rats fed a standard diet served as the negative control (NC) group. A model of lipid metabolism disorder in rats was established by HFD feeding. The 32 rats fed a HFD were randomized into four groups (n = 8): (I) a high-fat diet (HFD) group; (II) an Essentiale Forte N treatment group (EF, positive control, 196.3 mg/kg); (III) a low-dose oroxin A treatment group (LA, 50 mg/kg); and (IV) a high-dose oroxin A treatment group (HA, 200 mg/kg). In addition, the rats in both the CON and HFD groups were randomly administered vehicle (0.5% CMC-Na) by gavage every day for 3 months.

2.5.3. Experiment 2

Eight rats fed a standard diet served as the negative control group (NC2). Disordered lipid metabolism was induced in rats by HFD feeding, and the 48 rats fed a high-fat diet were randomized into six groups (n = 8): (I) the high-fat diet group (HFD2); (II) the high-dose oroxin A treatment group (HA2, 200 mg/kg); (III) the low-dose atorvastatin treatment group (AT(10), 10 mg/kg/d); (IV) the high-dose atorvastatin treatment group (AT(30), 30 mg/kg/d); (V) the low-dose atorvastatin and oroxin A combination treatment group (AT (10) + HA); and (VI) the high-dose atorvastatin and oroxin A combination treatment group (AT(30) + HA). Furthermore, the rats in both the CON and HFD groups were randomly administered vehicle (0.5% CMC-Na) by gavage every day for 3 months.

2.5.4. Physiological and biochemical properties

In the last week of the animal experiments, food intake was assayed. All rats were euthanized by isoflurane inhalation. In addition, we recorded the premortem weight of each group of rats and collected blood and liver samples for processing and preservation until further analysis. The plasma levels of fasting plasma glucose (FPG), 2-h postprandial glucose (2h-PG), TC, TG, LDLC, HDLC, ALT, and

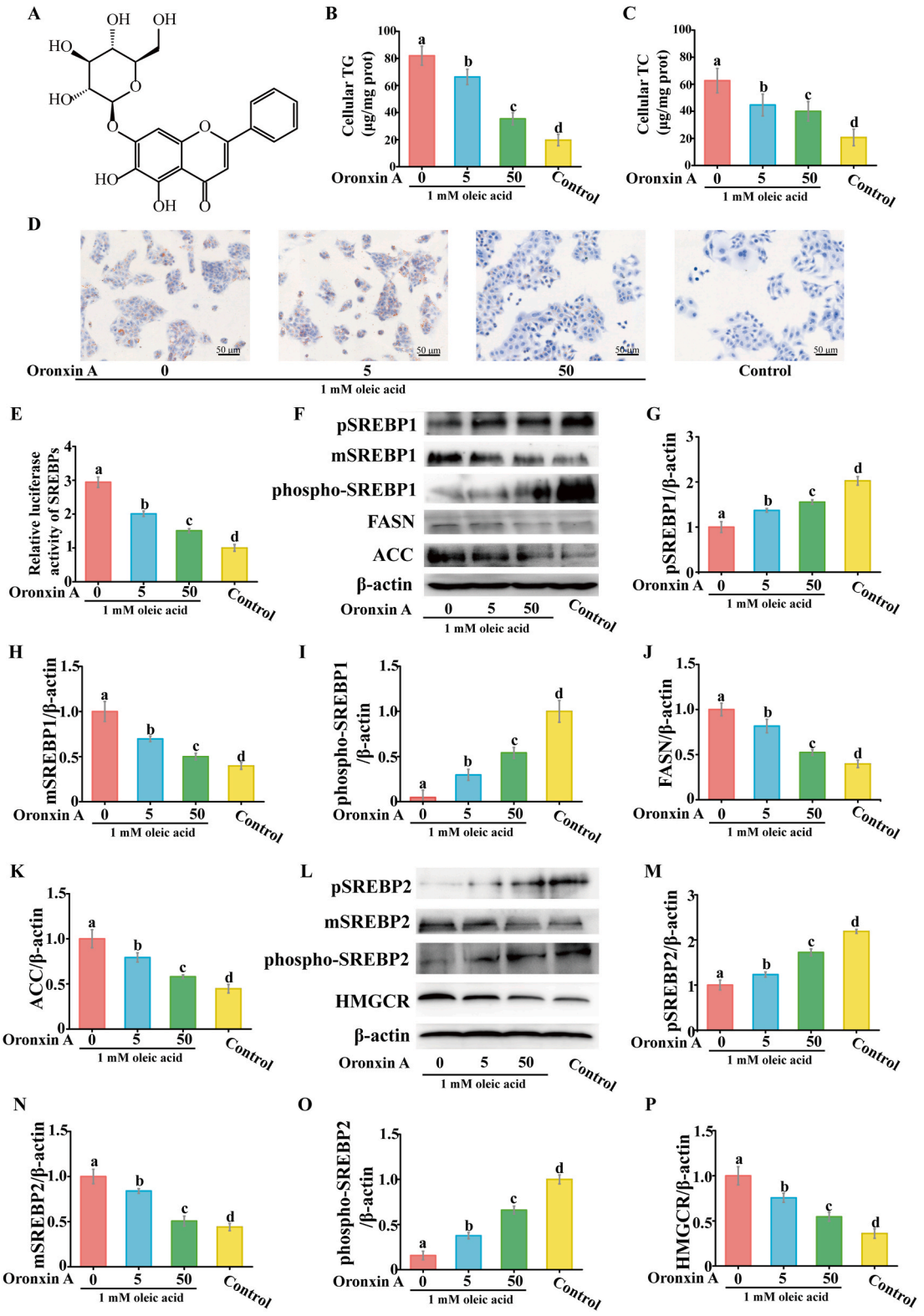

Fig. 1. Effects of oroxin A on lipid accumulation, SREBPs, the SREBP1 pathway, and the SREBP2 pathway in oleic acid-induced fatty HepG2 cells. (A) Structure of oroxin A. (B) Cellular TG levels. (C) Cellular TC levels. (D) Oil Red O staining. (E) Transcriptional activity of SREBPs. (F) Immunoblot analysis of pSREBP1, mSREBP1, phospho-SREBP1, FASN and ACC. (G) Densitometric analysis of pSREBP1. (H) Densitometric analysis of mSREBP1. (I) Densitometric analysis of phospho-SREBP1. (J) Densitometric analysis of FASN. (K) Densitometric analysis of ACC. (L) Immunoblot

analysis of pSREBP2, mSREBP2, phospho-SREBP2 and HMGCR. (M) Densitometric analysis of pSREBP2. (N) Densitometric analysis of mSREBP2. (O) Densitometric analysis of phospho-SREBP2. (P) Densitometric analysis of HMGCR. The data are presented as the means ± standard deviations (n = 3 for each group). The significance of the differences ($P < 0.05$) was analysed by one-way ANOVA followed by the LSD test for multiple comparisons. The values sharing a common letter (a, b, c, and d) were not significantly different ($P > 0.05$). (For interpretation of the references to colour in this figure legend, the reader is referred to the Web version of this article.)

AST were assayed using commercial kits according to the instructions. Additionally, the TC and TG levels in hepatic tissues were also analysed using commercial kits according to the instructions.

2.5.5. *In vivo* immunoblot analysis

For *in vivo* immunoblot analyses, protein samples were excised from the hepatic tissues of all groups of rats in Experiment 1, and the abundances of phospho-SREBP1, pSREBP1, mSREBP1, phospho-SREBP2, SREBP2, AMPK, pAMPK, ACC, FASN, HMGCR, and β-actin were analysed as described above.

2.5.6. *Histological analysis*

Liver tissue samples from the rats in each group in Experiment 1 were excised, fixed in formalin solution and embedded in paraffin to prepare 3-μm paraffin sections. The sections were then stained with haematoxylin-eosin or Oil Red O and observed at an appropriate magnification of 40× .

2.5.7. *In vivo immunofluorescence staining*

In vivo immunofluorescence staining was performed as described previously with minor modifications [19]. The washes mentioned in the following steps were performed with PBS for 3 min. The steps were the following. (1) Dewaxing and hydration: after baking at 65 °C for 1 h, the antigens were dewaxed twice by xylene immersion for 10 min each time, and this step was followed by hydration of the samples in 100%, 100%, 95%, 85% and 75% ethanol for 2 min, washing twice with distilled water for 3 min each time, and washing with PBS for 3 min. 2) Repair of antigens: the antigens were subjected to high-pressure heat treatment with EDTA repair solution for 2.5 min, and after natural cooling, the samples were washed 3 times. 3) Closure of endogenous peroxidase: 3% hydrogen peroxide was added to the sample, and the mixture was culture for 10 min at room temperature and then washed 3 times. 4) Closure: animal serum was added, and the samples were sealed at 37 °C for 10 min. 5) Primary antibody incubation: after removal of the blocking solution, anti-SREBP1/anti-SREBP2 antibodies (1:100) were added, and the samples were cultured overnight at 4 °C and then washed 3 times. 6) Secondary antibody incubation: after incubation with FITC-labelled secondary antibody (30 min at 37 °C) at 4 °C for 1 h, the samples were washed 3 times. 7) Dehydration: the samples were dehydrated in 75%, 85%, 95% and 100% ethanol for 2 min and then immersed in xylene twice for 2 min each. 8) Staining and sealing: the nuclei were stained with DAPI, and the samples were sealed with neutral gel and observed under a microscope (Olympus IX81). When SREBP1 or SREBP2 underwent nuclear translocation, a FITC fluorescence signal was observed in the DAPI-stained nuclei for the quantification of SREBP1 or SREBP2.

2.6. *Statistical analyses*

SPSS 17.0 was used for the statistical analyses, and both the *in vitro* and *in vivo* experimental results are expressed as the means ± standard deviations. The significance level of the differences ($P < 0.05$) was analysed by one-way ANOVA, and the least significant difference (LSD) test was used for multiple comparisons. In addition, different letters (a, b, c) in the corresponding graphs or tables indicate statistically significant differences ($P < 0.05$).

3. Results

3.1. *Oroxin a reduced lipid accumulation in oleic acid-induced fatty HepG2 cells*

The structure of oroxin A is shown in Fig. 1A. The levels of TC, TG and lipid accumulation were significantly increased in the fatty HepG2 cells induced by 1 mM oleic acid ($P < 0.01$ and $P < 0.001$) (Fig. 1B–D). In contrast, oroxin A decreased the cellular TG and TC levels in a dose-dependent manner ($P < 0.05$ for 5 μM oroxin A and $P < 0.001$ for 50 μM oroxin A) (Fig. 1B and C). These data indicated that oroxin A might reduce fatty acid synthesis and cholesterol synthesis. Furthermore, oroxin A reduced the area of Oil Red O staining (Fig. 1D). Taken together, these data indicate that oroxin A could inhibit oleic acid-induced cellular lipid accumulation.

3.2. *Oroxin a inhibited the transcriptional activity of SREBPs*

The transcriptional activity of SREBPs in HepG2 cells was determined by a dual-luciferase system, and the results revealed that the activity was significantly increased by oleic acid. Oroxin A significantly inhibited the increase in SREBP transcription in a dose-dependent manner ($P < 0.001$), and 50 μM oroxin A exerted the strongest effect ($P < 0.001$) (Fig. 1E).

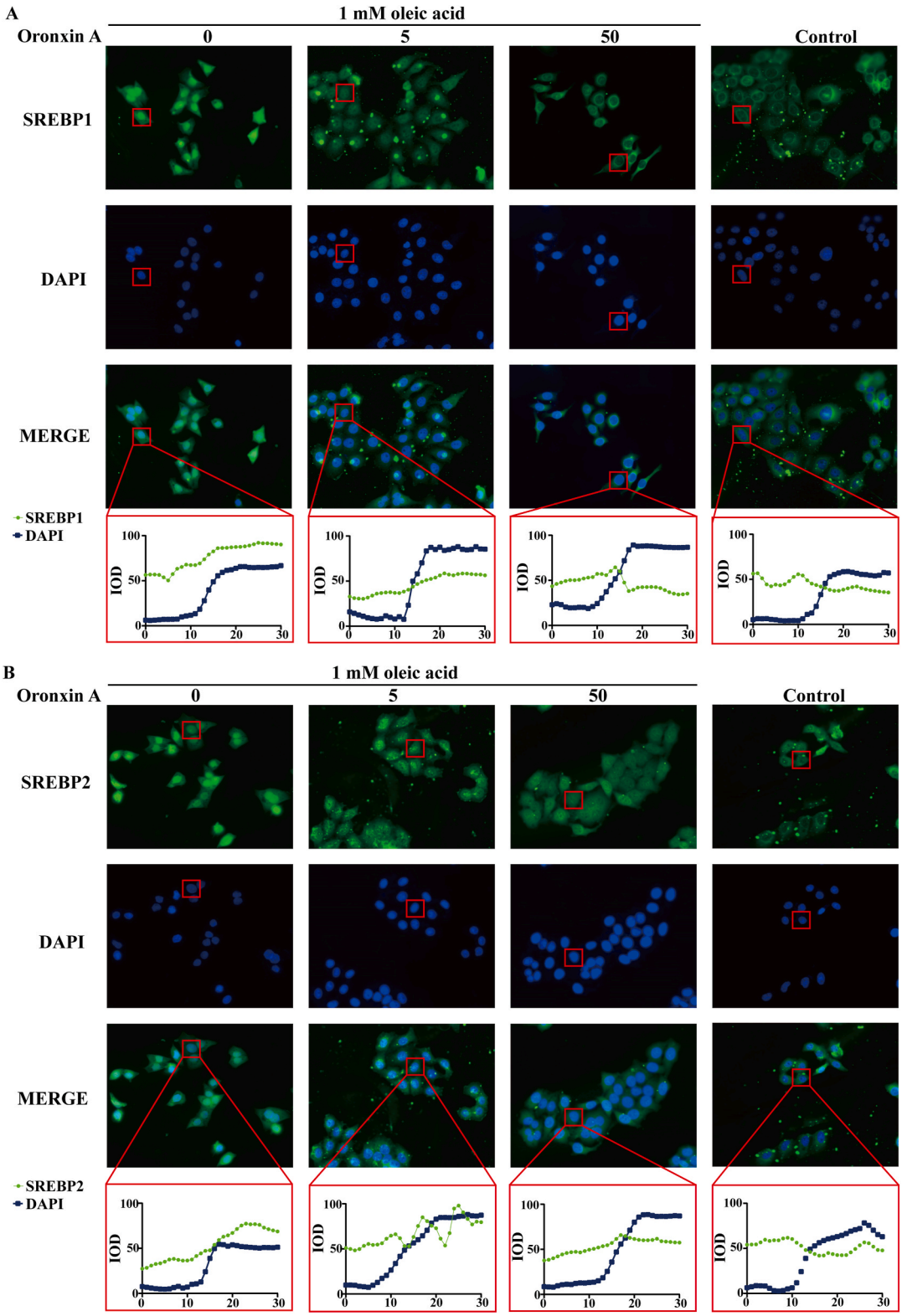

Fig. 2. Effects of oroxin A on SREBP1 and SREBP2 in oleic acid-induced fatty HepG2 cells evaluated by immunofluorescence. (A) Immunofluorescence analysis of DAPI and SREBP1; merged image of DAPI and SREBP1; and relative luminance curves of DAPI and SREBP1 in a representative area (from the edge to the centre of the marked yellow frame). (B) Immunofluorescence analysis of DAPI and SREBP2; merged image of DAPI and SREBP2; and relative luminance curves of DAPI and SREBP2 in a representative area (from the edge to the centre of the marked yellow frame). The

data are presented as the means ± standard deviations (n = 3 for each group). The significance of the differences ($P < 0.05$) was analysed by one-way ANOVA followed by the LSD test for multiple comparisons. The values sharing a common letter (a, b, c, and d) were not significantly different ($P > 0.05$). (For interpretation of the references to colour in this figure legend, the reader is referred to the Web version of this article.)

3.3. Oroxin a inhibited the SREBP1-related signalling pathway in vitro

We treated HepG2 cells with high concentrations of oleic acid to establish a fatty HepG2 cell model. To determine the effect of oroxin A on the SREBP1-related signalling pathway, the cells were treated with oroxin A for 24 h or with phospho-SREBP1 for 6 h. The results showed that oroxin A elevated the phosphorylation level of SREBP1 ($P < 0.05$) and the expression level of pSREBP1 ($P < 0.01$) and reduced the expression level of mSREBP1 ($P < 0.05$) (Fig. 1F–I). Similarly, treatment with oroxin A for 24 h reduced the expression levels of ACC and FASN ($P < 0.05$) (Fig. 1F–J and K). All of the abovementioned results showed a dose-dependent effect. In addition, immunofluorescence analysis revealed that oroxin A treatment increased the amount of SREBP1 in the cytoplasm and decreased the amount in the nucleus (Fig. 2A).

3.4. Oroxin a inhibited the SREBP2-related signalling pathway in vitro

We treated fatty HepG2 cells with oroxin A for 24 h or phospho-SREBP2 for 6 h and found that oroxin A elevated the cellular phosphorylation level of SREBP2 ($P < 0.01$) and the expression level of pSREBP2 ($P < 0.05$) and reduced the expression level of mSREBP2 ($P < 0.05$) (Fig. 1L-O). Moreover, treatment with oroxin A for 24 h reduced the expression level of HMGCR ($P < 0.05$) (Fig. 1L and P). In addition, immunofluorescence analysis indicated that oroxin A increased the amount of SREBP2 in the cytoplasm and reduced the amount in the nucleus (Fig. 2B).

3.5. Oroxin a inhibited the SREBP-related signalling pathway by phosphorylating AMPK

To further confirm the mechanism by which oroxin A inhibits SREBP transcriptional activity, we determined the phosphorylation levels of several signalling proteins. We found that 50 μM oroxin A increased the phosphorylation level of AMPK ($P < 0.01$) (Fig. 3A).

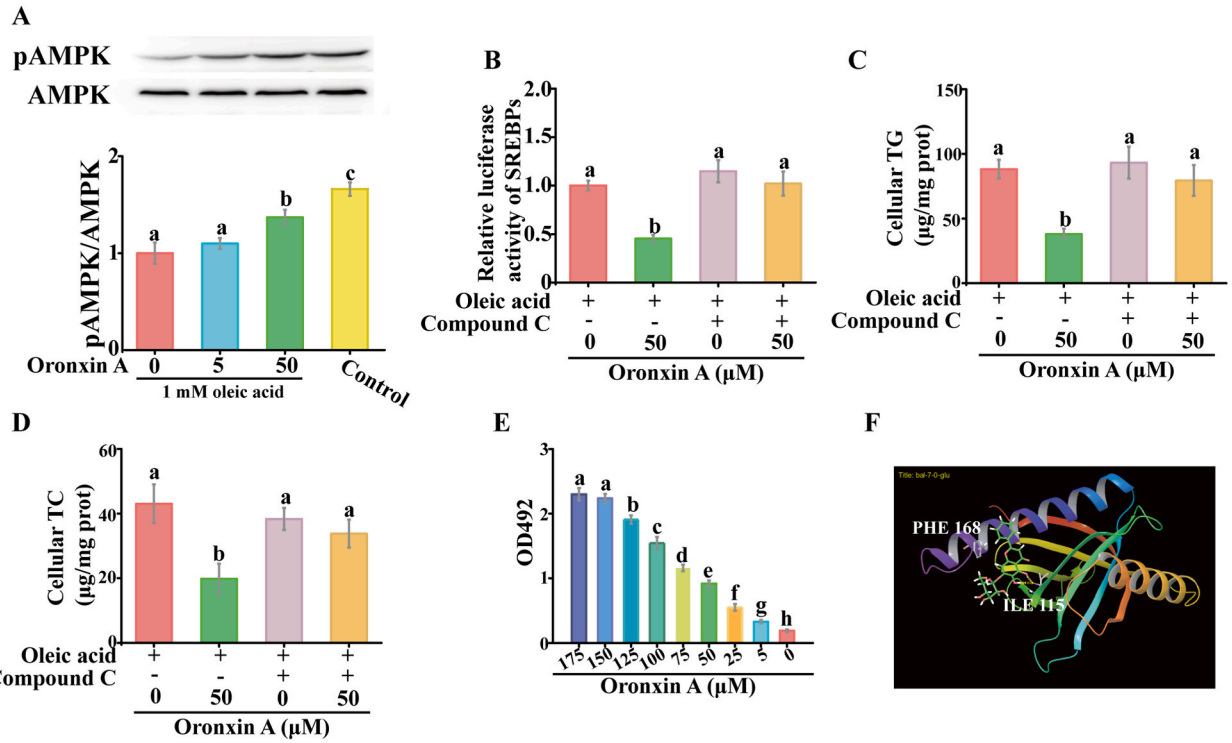

Fig. 3. Effect of oroxin A on the AMPK and LDLR levels in oleic acid-induced fatty acid-treated HepG2 cells. (A) Immunoblot and densitometric analysis of pAMPK and AMPK. (B) Transcriptional activity of SREBPs. (C) Cellular TG levels. (D) Cellular TC levels. (E) Binding of oroxin A to LDLR. (F) Docking of LDLR to oroxin A. The data are presented as the means ± standard deviations (n = 3 for each group). The significance of the differences ($P < 0.05$) was analysed by one-way ANOVA followed by the LSD test for multiple comparisons. The values sharing a common letter (a, b, c, and d) were not significantly different ($P > 0.05$). (For interpretation of the references to colour in this figure legend, the reader is referred to the Web version of this article.)

Furthermore, to determine the regulatory mechanism of oroxin A, the cells were treated with DMSO (control), oroxin A (50 μM), compound C (dorsomorphin, an AMPK phosphorylation inhibitor, 10 μM) or a combination of compound C and oroxin A (Fig. 3B). The results indicated that compound C treatment significantly increased the transcriptional activity of SREBP compared with that obtained with oroxin A treatment ($P < 0.001$). Moreover, compared with the levels observed after oroxin A treatment, compound C treatment elevated the cellular TC and TG levels (both $P < 0.01$) (Fig. 3C and D). These data indicate that oroxin A can inhibit the SREBP-related signalling pathway by phosphorylating AMPK.

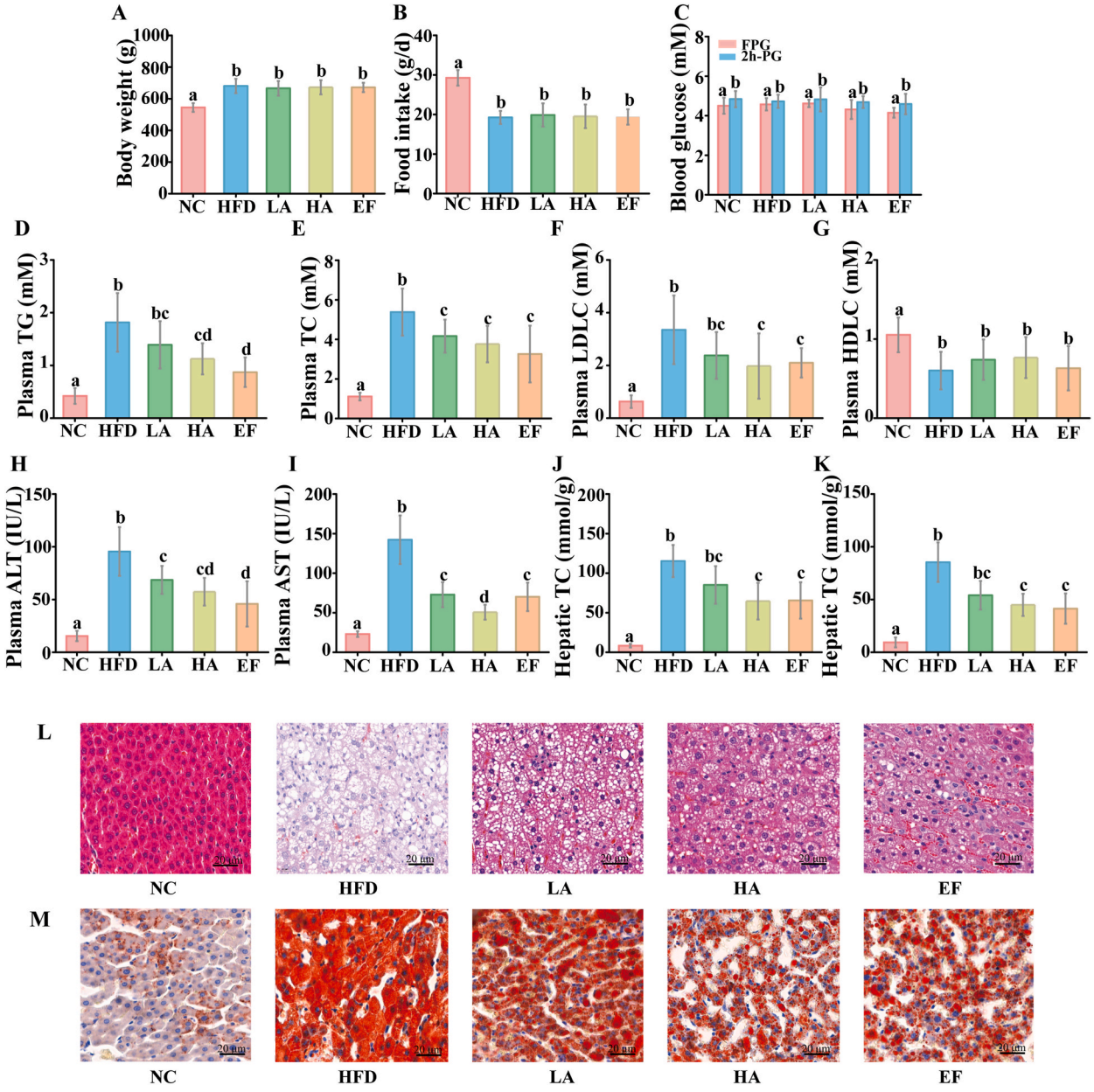

Fig. 4. Effects of oroxin A on the plasma lipid profile, hepatic lipid profile, and liver function, architecture, and morphology of HFD-fed rats. (A) Body weight. (B) Food intake. (C) Blood glucose. (D) Plasma TG. (E) Plasma TC. (F) Plasma LDLC. (G) Plasma HDLC. (H) Plasma ALT. (I) Plasma AST. (J) Hepatic TC. (K) Hepatic TG. (L) HE staining of the liver. (M) Oil Red O staining of the liver. NC: rats fed the standard chow and administered 0.5% CMC-Na; HFD: rats fed the HFD chow and administered 0.5% CMC-Na; LA: rats fed the HFD chow and administered 50 mg/kg/d oroxin A in 0.5% CMC-Na; HA: rats fed the HFD chow and administered 200 mg/kg/d oroxin A in 0.5% CMC-Na; EF: rats fed the HFD chow and administered 196.3 mg/kg Essentiale Forte N in 0.5% CMC-Na. The data are presented as the means ± standard deviations ($n = 8$ for each group). The significance of the differences ($P < 0.05$) was analysed by one-way ANOVA followed by the LSD test for multiple comparisons. The values sharing a common letter (a, b, c, and d) were not significantly different ($P > 0.05$). (For interpretation of the references to colour in this figure legend, the reader is referred to the Web version of this article.)

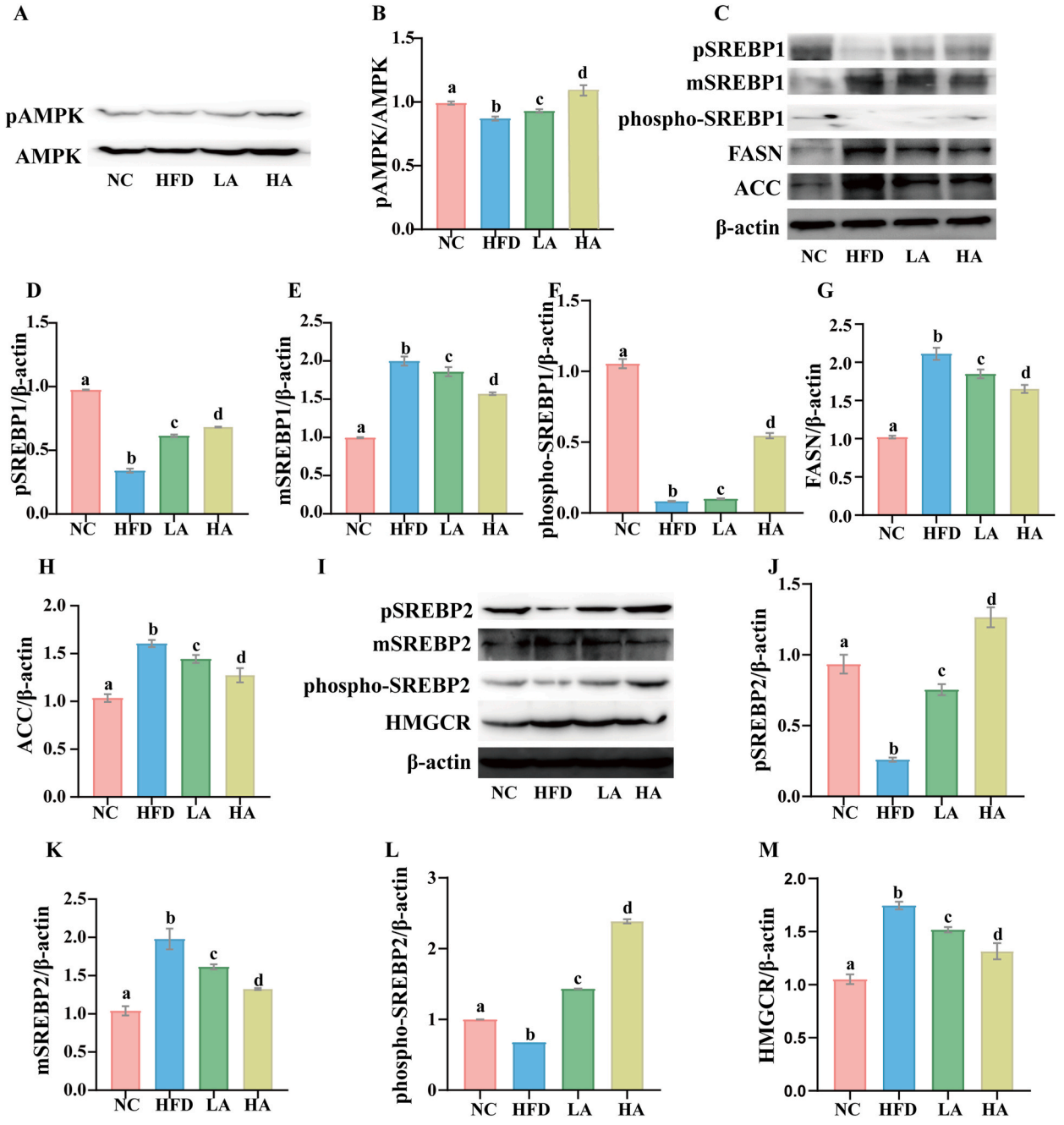

Fig. 5. Effects of oroxin A on the AMPK/SREBP pathway in HFD-fed rats. (A) Immunoblot analysis of pAMPK and AMPK. (B) Densitometric analysis of pAMPK and AMPK. (C) Immunoblot analysis of pSREBP1, mSREBP1, phospho-SREBP1, FASN and ACC. (D) Densitometric analysis of pSREBP1. (E) Densitometric analysis of mSREBP1. (F) Densitometric analysis of phospho-SREBP1. (G) Densitometric analysis of FASN. (H) Densitometric analysis of ACC. (I) Immunoblot analysis of pSREBP2, mSREBP2, phospho-SREBP2 and HMGCR. (J) Densitometric analysis of pSREBP2. (K) Densitometric analysis of mSREBP2. (L) Densitometric analysis of phospho-SREBP2. (M) Densitometric analysis of HMGCR. NC: rats fed the standard chow and administered 0.5% CMC-Na; HFD: rats fed the HFD chow and administered 0.5% CMC-Na; LA: rats fed the HFD chow and administered 50 mg/kg/d oroxin A in 0.5% CMC-Na; HA: rats fed the HFD chow and administered 200 mg/kg/d oroxin A in 0.5% CMC-Na. The data are presented as the means ± standard deviations (n = 8 for each group). The significance of the differences ($P < 0.05$) was analysed by one-way ANOVA followed by the LSD test for multiple comparisons. The values sharing a common letter (a, b, c, and d) were not significantly different ($P > 0.05$). (For interpretation of the references to colour in this figure legend, the reader is referred to the Web version of this article.)

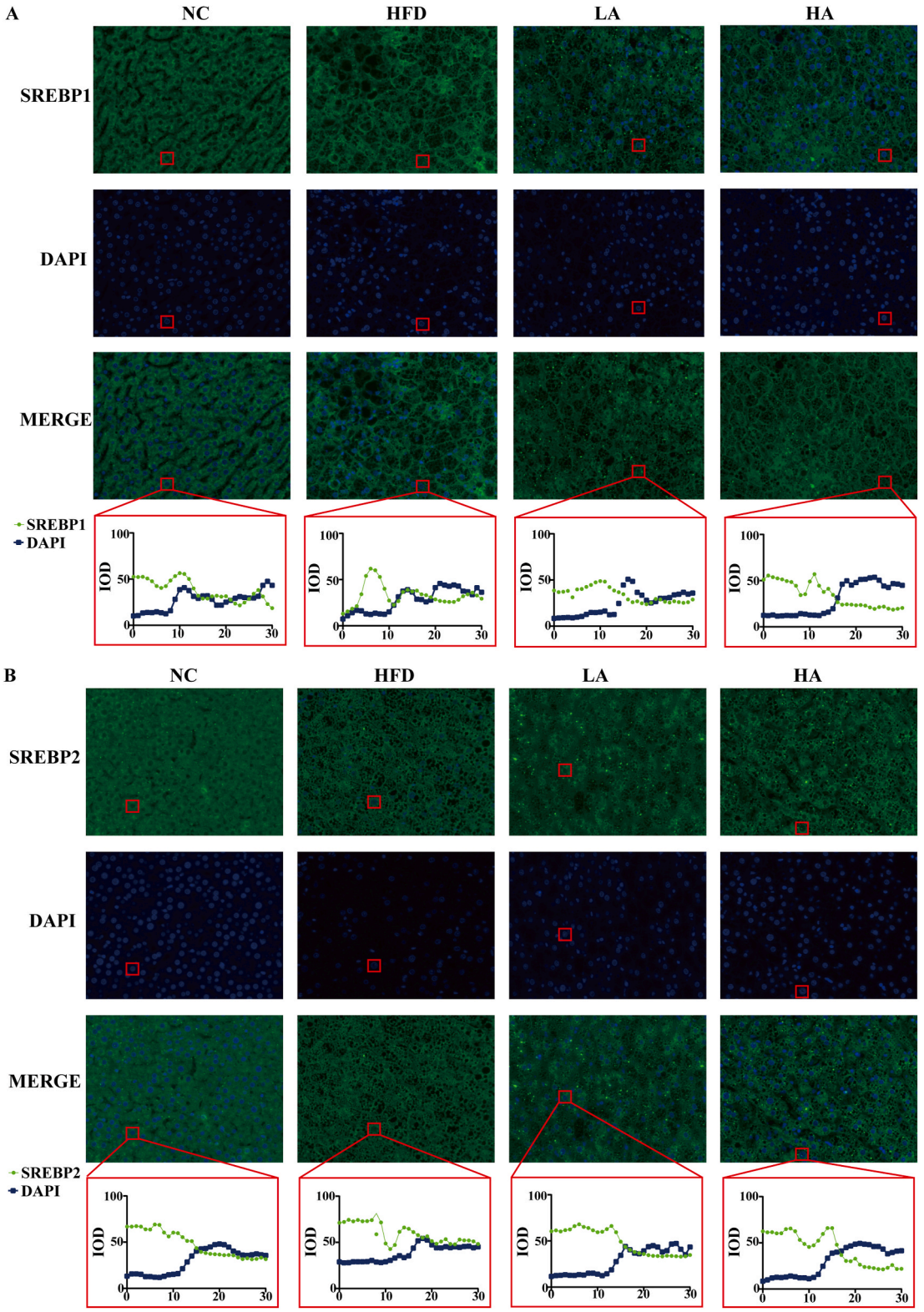

Fig. 6. Effect of oroxin A on SREBP1 and SREBP2 in the livers of HFD-fed rats evaluated by immunofluorescence. (A) Immunofluorescence analysis of DAPI and SREBP1; merged image of DAPI and SREBP1; and relative luminance curves of DAPI and SREBP1 in a representative area (from the edge to the centre of the marked yellow frame). (B) Immunofluorescence analysis of DAPI and SREBP2; merged image of DAPI and SREBP2; and relative luminance curves of DAPI and SREBP2 in a representative area (from the edge to the centre of the marked yellow frame). NC: rats fed the standard

chow and administered 0.5% CMC-Na; HFD: rats fed the HFD chow and administered 0.5% CMC-Na; LA: rats fed the HFD chow and administered 50 mg/kg/d oroxin A in 0.5% CMC-Na; HA: rats fed the HFD chow and administered 200 mg/kg/d oroxin A in 0.5% CMC-Na. The data are presented as the means ± standard deviations (n = 8 for each group). The significance of the differences ($P < 0.05$) was analysed by one-way ANOVA followed by the LSD test for multiple comparisons. The values sharing a common letter (a, b, c, and d) were not significantly different ($P > 0.05$). (For interpretation of the references to colour in this figure legend, the reader is referred to the Web version of this article.)

3.6. Oroxin a might regulate the phosphorylation of AMPK by binding to the LDLR protein

We evaluated the binding of the receptor protein to oroxin A by ELISA and detected tight interactions between the LDLR protein and oroxin A. The binding of LDLR to oroxin A was significantly increased by increases in the oroxin A concentrations ($P < 0.01$) (Fig. 3E). Furthermore, we used Schrodinger Maestro 9.4 to predict the site in LDLR that binds to oroxin A. Oroxin A was observed to bind to residues Phe168 and Ile115 of LDLR via two hydrogen bonds, and these strong interactions served as the foundation of oroxin A-LDLR binding (Fig. 3F).

3.7. Oroxin a improved the plasma lipid profile of HFD-fed non-IR rats

Only the rats in the HFD and NC groups exhibited different weights, and the weight of the HFD group was significantly greater than that of the NC group ($P < 0.001$) (Fig. 4A). In contrast, no differences in body weight or food intake were found among the HFD, LA and HA groups ($P > 0.05$) (Fig. 4B). In addition, no difference in FPG or 2h-PG was detected between the HFD and NC groups ($P > 0.05$), which indicated that the HFD did not induce an increase in blood glucose or insulin resistance, and no difference in FPG or 2h-PG was found among the HFD, LA, and HA groups ($P > 0.05$) (Fig. 4C). HFD feeding for 3 months significantly increased the TC, TG and LDLC levels and significantly reduced the HDLC level ($P < 0.01$) (Fig. 4D–G). However, a significant improvement in the plasma lipid profile was observed after treatment with oroxin A or EF. Although it did not change the HDLC level, oroxin A significantly decreased the TC, TG, and LDLC levels ($P < 0.05$) (Fig. 4D–G).

3.8. Oroxin a improved the function, hepatic lipid profile, and morphology of HFD-fed non-IR rats

Administration of a HFD for 3 months significantly increased the ALT and AST levels ($P < 0.001$), and oroxin A or EF treatment

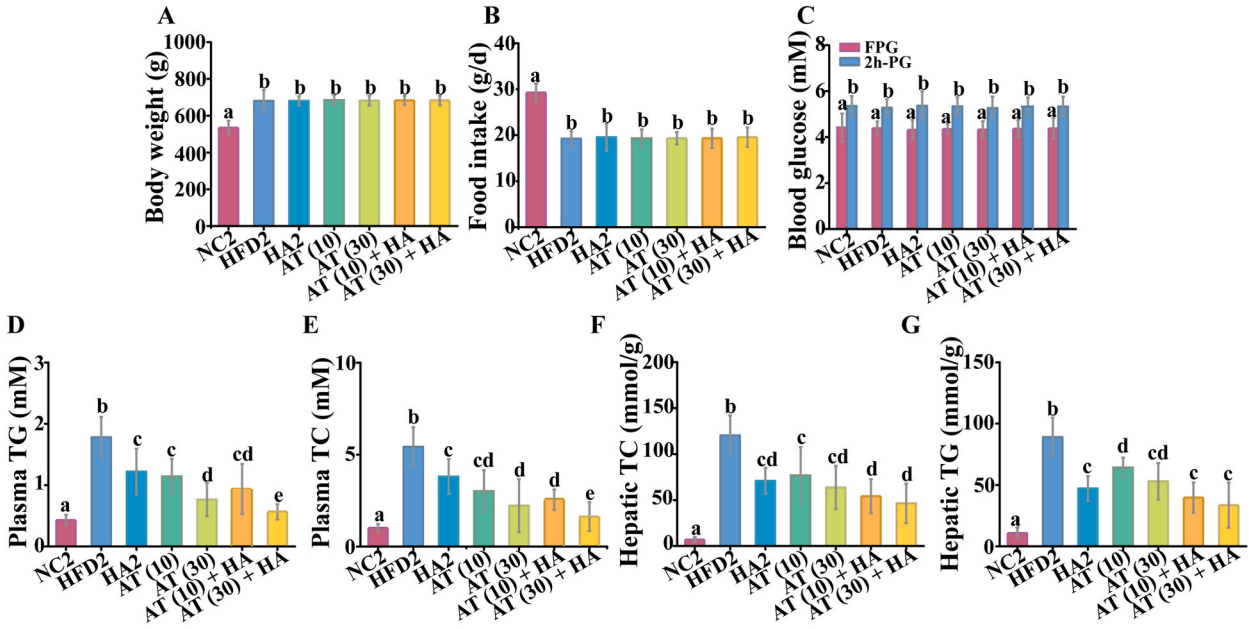

Fig. 7. Effects of oroxin A combined with atorvastatin on the plasma lipid profile of HFD-fed rats. (A) Body weight. (B) Food intake. (C) Blood glucose. (D) Plasma TG. (E) Plasma TC. (F) Hepatic TC. (G) Hepatic TG. NC2: rats fed the standard chow and administered 0.5% CMC-Na; HFD2: rats fed HFD chow were administered 0.5% CMC-Na; HA2: rats fed the HFD chow and administered 200 mg/kg/d oroxin A in 0.5% CMC-Na; AT (10): rats fed the HFD chow and administered 10 mg/kg/d atorvastatin in 0.5% CMC-Na; AT (30): rats fed the HFD chow and administered 30 mg/kg/d atorvastatin in 0.5% CMC-Na; AT (10) + HA: rats fed the HFD chow and administered 10 mg/kg/d atorvastatin and 200 mg/kg/d oroxin A in 0.5% CMC-Na; AT (30) + HA: rats fed the HFD chow and administered 30 mg/kg/d atorvastatin and 200 mg/kg/d oroxin A in 0.5% CMC-Na. The data are presented as the means ± standard deviations (n = 8 for each group). The significance of the differences ($P < 0.05$) was analysed by one-way ANOVA followed by the LSD test for multiple comparisons. The values sharing a common letter (a, b, c, and d) were not significantly different ($P > 0.05$). (For interpretation of the references to colour in this figure legend, the reader is referred to the Web version of this article.)

significantly reduced the ALT and AST levels ($P < 0.05$ or $P < 0.001$) (Fig. 4H and I), suggesting that oroxin A can improve hepatic function. In addition, the hepatic TC and TG levels were also significantly increased after HFD feeding for 3 months ($P < 0.001$), and oroxin A or EF significantly reduced the TC and TG levels ($P < 0.001$ or $P < 0.001$), indicating that oroxin A can reduce the hepatic lipid profile (Fig. 4J and K). Morphological observations revealed that HFD feeding for 3 months induced cellular swelling and a significant increase in the number of large and/or small hollow spaces, but oroxin A or EF reversed this damage, suggesting that oroxin A largely restored the structure and morphology of the liver (Fig. 4L). Additionally, the area of Oil Red O staining increased after HFD feeding for 3 months, but oroxin A or EF reversed this change, which indicated that oroxin A can reduce lipid accumulation in the liver (Fig. 4M).

3.9. Oroxin a inhibited the SREBP-related signalling pathway in vivo

The results indicated that oroxin A treatment for 3 months increased the level of AMPK phosphorylation ($P < 0.01$) (Fig. 5A and B). Furthermore, oroxin A elevated the phosphorylation level of SREBP1 ($P < 0.01$) and the expression level of pSREBP1 ($P < 0.001$) and reduced the expression levels of mSREBP1, ACC and FASN ($P < 0.05$) (Fig. 5C–H). Similarly, oroxin A also elevated the phosphorylation level of SREBP2 ($P < 0.001$) and the expression level of pSREBP2 ($P < 0.001$) and decreased the expression levels of mSREBP2 and HMGCR ($P < 0.05$) (Fig. 5I-M). Furthermore, immunofluorescence analysis indicated that oroxin A increased the amounts of SREBP1 and SREBP2 in the cytoplasm and reduced the amounts in the nucleus (Fig. 6A and B).

3.10. Oroxin a enhanced the lipid-lowering effect of atorvastatin

Treatment with both oroxin A and atorvastatin for 3 months did not change the body weight, food intake, and blood glucose levels compared with those observed after treatment with oroxin A or atorvastatin alone ($P > 0.05$) (Fig. 7A–C). Furthermore, the examination of the plasma lipid profiles showed that treatment with both oroxin A and atorvastatin significantly decreased the TC and TG levels compared with those measured after treatment with oroxin A or atorvastatin alone ($P < 0.01$) (Fig. 7D and E). Additionally, the analysis of the hepatic lipid profiles revealed that the combined treatment decreased the TC and TG levels compared with those observed after treatment with oroxin A or atorvastatin alone, although the differences were not significant ($P > 0.05$) (Fig. 7F and G).

4. Discussion

Lipid metabolism disorders have become a major global public health issue, and more effective approaches for adjusting to different patient conditions are needed. Although chemically synthesized drugs exert definite effects on dyslipidaemia, most of these drugs can have additional side effects if used for a long period. For example, high doses of statins may not significantly increase the hypolipidaemic effects but may cause liver damage, gastrointestinal dysfunction and renal impairment [5]. Therefore, the identification of safe and effective drugs that can improve lipid metabolism disorders is important. In preliminary experiments, we performed toxicity tests to determine the optimal experimental dose of oroxin A and found that treatment with 0–2 g/kg oroxin A for 2 weeks failed to cause mortality in rats and that 3 g/kg oroxin A caused slight behavioural changes in rats (data not shown). Therefore, we considered an oroxin A dose of 2 g/kg to be safe for rats and selected 200 mg/kg/d oroxin A (a dose equal to 1/10 of this safe dose) as the experimental dose to be used in this study. Furthermore, in our previous studies, many flavonoids, such as hesperetin and baicalin, exerted hypolipidaemic effects when given at high doses (200 mg/kg/d), whereas low doses (50 or 100 mg/kg/d) also tended to have effects [8,9,13]. Therefore, doses of 50 mg/kg/d and 200 mg/kg/d were used in our subsequent animal experiments. In this study, our results showed that oroxin A could ameliorate lipid metabolism disorders under non-IR conditions, which was similar to the results obtained with EF; specifically, oroxin A could reduce the plasma and hepatic lipid profiles, ameliorate NAFLD, and enhance the lipid-lowering effect of atorvastatin. Our results also indicated that oroxin A could inhibit the transcriptional activity of SREBP1 and SREBP2. Furthermore, oroxin A reduced the TG levels by inhibiting SREBP1 and decreasing the TC levels through inhibition of SREBP2. Further results indicated that oroxin A could bind to LDLR and increase AMPK phosphorylation, which might be the mechanism by which oroxin A regulates SREBPs. These new findings indicate the value of oroxin A in the control of lipid metabolism disorders and may reveal new pharmacological mechanisms for the treatment of lipid metabolism disorders; this mechanistic information is expected to provide a basic theory for the clinical treatment of lipid metabolism disorders.

An increasing number of studies have shown the advantages of natural products in the treatment of chronic metabolic diseases such as lipid metabolism disorders. Flavonoids have received widespread attention due to their multiple pharmacological activities, such as antioxidant, anti-inflammatory, hepatoprotective, and free radical scavenging activities [20]. Natural flavonoids such as hesperidin, hesperetin, naringin, naringenin, apigenin and quercetin have been found to potentially regulate lipid or cholesterol metabolism [21]. Furthermore, citrus flavonoids, including naringenin, hesperidin, nobiletin and tangeretin, have emerged as natural lead compounds for the treatment of lipid metabolism diseases by preventing hepatic steatosis, dyslipidaemia, and insulin sensitivity, mainly through the inhibition of hepatic fatty acid synthesis and increased fatty acid oxidation [22]. The total flavonoids of *Perilla frutescens* leaves, which mainly consists of apigenin and a small amount of lignans, and the total flavonoids from blueberry leaves can effectively reduce the serum TC, TG, LDLC levels and adipose tissue lipid accumulation, increase the serum HDLC levels, and regulate the metabolic disorders of lipoproteins in rats fed a HFD [23,24]. Similarly, flavonoids extracted from *Apium graveolens* L. roots are able to reduce the lipid levels in a hyperlipidaemic rat model induced by high-fat emulsion feeding through decrease in the levels of cholesterol synthesis-related target proteins, including SREBP1, HMGCR, and ACC1 [25]. The present study showed that oroxin A, a flavonoid, reduced the blood and liver lipids in HFD-fed rats, which supports the notion that flavonoid natural products ameliorate lipid metabolism disorders. Flavonoids derived from other natural products may exert similar beneficial effects. This study not only expands

the scope of oroxin A application, which is beneficial for the development of oroxin A, but also provides a possible theoretical basis for the application of other flavonoid natural products and new research ideas for the treatment of lipid metabolism disorders.

SREBPs, which are located in the endoplasmic reticulum, are intracellular cholesterol sensors that regulate the transcription of genes encoding lipid-related enzymes. SREBPs are also typical nuclear transcription factors [26]. In the resting state, the SREBP precursor protein is located in the cytoplasm. When activated, SREBP in the endoplasmic reticulum is further cleaved to form mSREBP, which is subsequently translocated to the nucleus, where it regulates the transcription of corresponding genes [27]. SREBPs are encoded by the SREBP-1 and SREBP-2 genes. SREBP1-c is expressed mainly in the liver, and SREBP1-a is translated from the SREBP1 gene and regulates the expression of genes that synthesize fatty acids and triglycerides, such as those encoding FASN and ACC [28]. ACC is the rate-limiting enzyme of fatty acid synthesis, and its overexpression can promote fat synthesis. Studies have shown that the ACC content in the adipose tissue and liver of obese individuals is significantly greater than that in the corresponding tissues of people with a normal weight. ACC catalyses the first step of fatty acid synthesis (i.e., acetyl coenzyme A carboxylation to synthesize malonyl-coenzyme A), and subsequently, malonyl-coenzyme A further synthesizes growing fatty acid chains under the action of an enzyme system responsible for fatty acid carbon chain extension [29]. FASN is a multifunctional enzyme that plays an important role in fatty acid synthesis by catalysing the de novo biosynthesis of long-chain saturated fatty acids starting from acetyl-CoA and malonyl-CoA [30]. Our results indicated that oroxin A decreased the nuclear transcription level of SREBP1 and the expression levels of ACC and FASN *in vivo* and *in vitro*, and these effects may describe the main mechanism by which oroxin A reduces the hepatic TG levels. Additionally, due to the circulation of lipids between the liver and blood, decreased hepatic TG levels lead to a reduction in the plasma TG level. SREBP2 is translated from the SREBP2 gene and regulates the expression of cholesterol synthesis-related genes, such as HMGCR [31]. Cholesterol in the human body is generated mainly by an endogenous pathway, and HMGCR, the rate-limiting enzyme in cholesterol synthesis, directly affects the rate of cholesterol synthesis and the amount of cholesterol in the body. Previous research has indicated that HMGCR-related gene mRNA expression is upregulated after hepatocyte steatosis. Increases in HMGCR and cholesterol synthesis in the liver can increase the systemic cholesterol level in the circulation [32]. Our results indicated that oroxin A decreased the nuclear transcription level of SREBP2 and the expression level of HMGCR *in vivo* and *in vitro*, and these effects constitute the main mechanism by which oroxin A can reduce the hepatic TC level. Similarly, due to the circulation of lipids between the liver and blood, decreased hepatic TC levels result in reduced plasma TC levels. In fact, HMGCR is the main target of statins, which inhibit HMGCR activity. However, when hyperlipidaemia occurs under severe conditions, high-dose statins do not exert a better lipid-lowering effect than low-dose statins [33]. To address this issue, a suitable drug for combination treatment with statins is needed. Oroxin A, which can reduce the abundance of HMGCR, might be useful in combination with statins. Our results suggest that the lipid-lowering effect of oroxin A in combination with atorvastatin is superior to that of oroxin A or atorvastatin alone. Hence, oroxin A might be a good choice for enhancing the therapeutic efficacy of statins.

To study the mechanism by which oroxin A regulates SREBPs, we explored the effect of oroxin A on a series of protein kinases. Our results indicated that oroxin A elevated the phosphorylation level of AMPK and that an AMPK phosphorylation inhibitor (compound C) reduced the inhibitory effect of oroxin A on SREBPs. The abovementioned findings suggest that AMPK is a key factor in the regulatory effect of oroxin A on SREBPs. Many other researchers have also reported a relationship between AMPK and SREBPs, supporting our results [34]. Furthermore, we measured the binding efficacy of oroxin A to many receptors related to lipid metabolism, and our results indicated tight binding between oroxin A and the LDLR protein. LDLR is a transmembrane glycoprotein that plays an important role in maintaining constant cholesterol levels [35]. Previous research has demonstrated that inhibition of the LDLR protein increased the phosphorylation of AMPK [36,37], which might be the mechanism by which oroxin A regulates AMPK/SREBPs. However, to our knowledge, the regulation of LDLR is very complicated, and LDLR can be regulated by many proteins, such as PPARγ and other protein kinases [38,39]. Thus, further determination of whether the binding of oroxin A to LDLR directly results in changes in the AMPK/SREBP pathway would be quite difficult. Considering these findings, oroxin A might regulate the AMPK/SREBP pathway by binding to the LDLR protein, but additional research is needed.

In the present study, we found that the LDLR/AMPK/SREBP signalling pathway is involved in the development of lipid metabolism disorders and may provide constitute a new pharmacological mechanism for ameliorating lipid metabolism disorders. These results suggest that oroxin A may be valuable for controlling lipid metabolism disorders and further support the notion that flavonoid natural products ameliorate lipid metabolism disorders. Second, the results of the present study also showed that oroxin A can enhance the therapeutic efficacy of statins, and these findings provide a theoretical basis for the clinical treatment of lipid metabolism disorders, which is expected to become a new research direction. This study has several limitations. On the one hand, our study focused on the modulatory role of SREBPs in the lipid-lowering effect of oroxin A. The antioxidant activity of oroxin A might also be beneficial for the prevention and treatment of lipid metabolism disorders [40]. On the other hand, although we investigated the binding of oroxin A to LDLR, whether both of these proteins play direct roles in the lipid-lowering effect of oroxin A remains to be determined and warrants further study.

5. Conclusion

In conclusion, oroxin A significantly improved disordered lipid metabolism and the plasma lipid profile in patients with hyperlipidaemia under normal conditions, enhanced the lipid-lowering effect of statins in the treatment of severe hyperlipidaemia, improved liver function and reduced hepatic lipid accumulation, indicating that it can be used for NAFLD treatment and prevention. Further mechanistic analysis indicated that oroxin A can inhibit the nuclear transcriptional activity of SREBPs to reduce lipid synthesis and that this effect might be regulated by the binding of oroxin A to the LDLR protein and increased phosphorylation of AMPK. Our research expands the range of *O. indicum* applications and supports the use of oroxin A as a natural lead compound for improving

disordered lipid metabolism. However, more detailed mechanistic and clinical studies are needed to establish appropriate applications of these materials.

Ethics approval

All animal handling procedures were performed in a standard laboratory and approved by the Institutional Animal Care and Use Committee of Shandong University of Technology (YLX20210801).

Funding

This work was supported by the Taishan Scholar Foundation of Shandong Province, China (tsqn202312184), the University Youth Innovation Team of Shandong Province, China (2022KJ229), the Natural Science Foundation of Shandong Province, China (ZR2022MH306), the Beijing Science and Technology New Star Project, China (Z201100000820027), and the National Key Research and Development Program, China (2022YFC2010104).

Data availability statement

WB raw data has been submitted as supplementary material. The other data sets used and analysed during the current study are available from the corresponding author upon reasonable request.

CRediT authorship contribution statement

Tianqi Cai: Writing – review & editing, Writing – original draft, Software, Methodology, Data curation. **Xiaoxue Xu:** Software, Methodology, Data curation. **Ling Dong:** Software, Methodology, Data curation. **Shufei Liang:** Software, Methodology, Data curation. **Meiling Xin:** Software, Methodology, Data curation. **Tianqi Wang:** Methodology, Data curation. **Tianxing Li:** Methodology, Data curation. **Xudong Wang:** Validation, Methodology. **Weilong Zheng:** Validation, Methodology. **Chao Wang:** Writing – review & editing, Writing – original draft, Data curation. **Zhengbao Xu:** Writing – review & editing, Writing – original draft, Data curation. **Meng Wang:** Writing – review & editing, Writing – original draft, Data curation. **Xinhua Song:** Writing – review & editing, Writing – original draft, Funding acquisition, Data curation. **Lingru Li:** Supervision, Project administration, Investigation, Funding acquisition. **Jingda Li:** Supervision, Project administration, Investigation. **Wenlong Sun:** Supervision, Project administration, Investigation, Funding acquisition.

Declaration of competing interest

The authors declare that they have no known competing financial interests or personal relationships that could have appeared to influence the work reported in this paper.

Acknowledgements

We are grateful to American Journal Experts for editing the English language of the manuscript.

Abbreviations

insulin-resistant (IR)
high-fat diet (HFD)
nonalcoholic fatty liver disease (NAFLD)
Food and Drug Administration (FDA)
total triglyceride (TG)
total cholesterol (TC)
high-density lipoprotein cholesterol (HDLC)
low-density lipoprotein cholesterol (LDLC)
aspartate transaminase (AST)
alanine transaminase (ALT)
polyvinylidene fluoride (PVDF)
Dulbecco's modified Eagle's medium (DMEM)
human hepatocellular carcinoma (HepG2)
low-density lipoprotein receptor (LDLR)
precursor sterol regulatory element-binding protein 1 (pSREBP1)
precursor sterol regulatory element-binding protein 2 (pSREBP2)
acetyl coenzyme A carboxylase (ACC)
acetyl coenzyme A carboxylase 1 (ACC1)

fatty acid synthase (FASN)
3-hydroxy-3-methylglutaryl-CoA reductase (HMGCR)
mature SREBP1 (mSREBP1)
mature SREBP2 (mSREBP2)
sterol regulatory element-binding protein 1 (SREBP1)
sterol regulatory element-binding protein 2 (SREBP2)
enzyme-linked immunosorbent assay (ELISA)
fasting plasma glucose (FPG)
2-h postprandial glucose (2h-PG)
least significant difference (LSD)

Appendix A. Supplementary data

Supplementary data to this article can be found online at https://doi.org/10.1016/j.heliyon.2024.e29168.

References

[1] B. Cariou, C.D. Byrne, R. Loomba, A.J. Sanyal, Nonalcoholic fatty liver disease as a metabolic disease in humans: a literature review, Diabetes Obes. Metabol. 23 (2021) 1069–1083.
[2] M.J. Ferrer, A.F. Silva, G.A. Abruzzese, M.E. Velázquez, A.B. Motta, Lipid metabolism and relevant disorders to female reproductive health, Curr. Med. Chem. 28 (27) (2021) 5625–5647.
[3] R. Guillamat-Prats, M. Rami, S. Herzig, S. Steffens, Endocannabinoid signalling in atherosclerosis and related metabolic complications, Thromb. Haemostasis 119 (2019) 567–575.
[4] F. Taroni, C. Gellera, Chapter 54 - disorders of lipid metabolism**This chapter is dedicated to the loving memory of Stefano Di Donato, MD (1940–2015), unforgettable mentor and friend, in: R.N. Rosenberg, J.M. Pascual (Eds.), Rosenberg's Molecular and Genetic Basis of Neurological and Psychiatric Disease, sixth ed., Academic Press, 2020, pp. 731–753.
[5] S. Sultan, A. D'Souza, I. Zabetakis, R. Lordan, A. Tsoupras, E.P. Kavanagh, N. Hynes, Chapter 6 - statins: rationale, mode of action, and side effects, in: I. Zabetakis, R. Lordan, A. Tsoupras (Eds.), The Impact of Nutrition and Statins on Cardiovascular Diseases, Academic Press, 2019, pp. 171–200.
[6] K. Wegermann, A.M. Diehl, C.A. Moylan, Disease pathways and molecular mechanisms of nonalcoholic steatohepatitis, Clin. Liver Dis. 11 (2018) 87–91.
[7] L. Nie, H. Song, A. He, S. Yao, Recent research progress in natural bioactive constituents against lipid metabolic diseases, Curr. Top. Med. Chem. 16 (23) (2016) 2605–2624.
[8] J. Li, T. Wang, P. Liu, F. Yang, X. Wang, W. Zheng, W. Sun, Hesperetin ameliorates hepatic oxidative stress and inflammation via the PI3K/AKT-Nrf2-ARE pathway in oleic acid-induced HepG2 cells and a rat model of high-fat diet-induced NAFLD, Food Funct. 12 (9) (2021) 3898–3918.
[9] W. Sun, P. Liu, T. Wang, X. Wang, W. Zheng, J. Li, Baicalein reduces hepatic fat accumulation by activating AMPK in oleic acid-induced HepG2 cells and high-fat diet-induced non-insulin-resistant mice, Food Funct. 11 (2020) 711–721.
[10] B. Dinda, I. SilSarma, M. Dinda, P. Rudrapaul, Oroxylum indicum (L.) Kurz, an important Asian traditional medicine: from traditional uses to scientific data for its commercial exploitation, J. Ethnopharmacol. 161 (2014) 255–278.
[11] J. He, L. Du, M. Bao, B. Zhang, H. Qian, Q. Zhou, Z. Cao, Oroxin A inhibits breast cancer cell growth by inducing robust endoplasmic reticulum stress and senescence, Anti Cancer Drugs 27 (3) (2015) 204–215.
[12] P. Sithisarn, P. Nantateerapong, P. Rojsanga, P. Sithisarn, Screening for antibacterial and antioxidant activities and phytochemical analysis of Oroxylum indicum fruit extracts, Molecules 21 (4) (2016) 446.
[13] W. Sun, B. Zhang, X. Yu, C. Zhuang, X. Li, J. Sun, Y. Xing, Z. Xiu, Y. Dong, Oroxin A from Oroxylum indicum prevents the progression from prediabetes to diabetes in streptozotocin and high-fat diet induced mice, Phytomedicine 38 (2018) 24–34.
[14] W. Sun, P. Liu, B. Yang, M. Wang, T. Wang, W. Sun, X. Wang, W. Zheng, X. Song, J. Li, A network pharmacology approach: inhibition of the NF-κB signaling pathway contributes to the NASH preventative effect of an Oroxylum indicum seed extract in oleic acid-stimulated HepG2 cells and high-fat diet-fed rats, Phytomedicine 88 (2021) 153498.
[15] W. Sun, Y. Sang, B. Zhang, X. Yu, Q. Xu, Z. Xiu, Y. Dong, Synergistic effects of acarbose and an Oroxylum indicum seed extract in streptozotocin and high-fat-diet induced prediabetic mice, Biomed. Pharmacother. 87 (2017) 160–170.
[16] J. Li, Z. Xiu, R. Wang, C. Yu, Y. Chi, J. Qin, C. Fu, E. Matsuura, Q. Liu, The lipid moiety 7-ketocholesteryl-9-carboxynonanoate mediates binding interaction of oxLDL to LOX-1 and upregulates ABCA1 expression through PPARγ, Life Sci. 177 (2017) 27–40.
[17] Y. Mi, D. Tan, Y. He, X. Zhou, Q. Zhou, S. Ji, Melatonin modulates lipid metabolism in HepG2 cells cultured in high concentrations of oleic acid: AMPK pathway activation may play an important role, Cell Biochem. Biophys. 76 (4) (2018) 463–470.
[18] J.G. Donaldson, Immunofluorescence staining, Curr. Protoc. Cell Biol. 69 (2015) 4.3.1–4.3.7.
[19] L. Panpan, W. Peixuan, Y. Bendong, W. Tianqi, L. Jingda, S. Xinhua, S. Wenlong, Kaempferol prevents the progression from simple steatosis to non-alcoholic steatohepatitis by inhibiting the NF-κB pathway in oleic acid-induced HepG2 cells and high-fat diet-induced rats, J. Funct.Foods 85 (2021) 104655.
[20] E. Middleton, C. Kandaswami, T.C. Theoharides, The effects of plant flavonoids on mammalian cells: implications for inflammation, heart disease, and cancer, Pharmacol. Rev. 52 (4) (2000) 673–751.
[21] E.F. Hoek-van den Hil, E.M. van Schothorst, I. van der Stelt, H.J.M. Swarts, M. van Vliet, T. Amolo, J.J.M. Vervoort, D. Venema, P.C.H. Hollman, I.M.C. M. Rietjens, J. Keijer, Direct comparison of metabolic health effects of the flavonoids quercetin, hesperetin, epicatechin, apigenin and anthocyanins in high-fat-diet-fed mice, Genes Nutr 10 (4) (2015) 469.
[22] J.M. Assini, E.E. Mulvihill, M.W. Huff, Citrus flavonoids and lipid metabolism, Curr. Opin. Lipidol. 24 (1) (2013) 34–40.
[23] L.-J. Feng, C.-H. Yu, K.-J. Ying, J. Hua, X.-Y. Dai, Hypolipidemic and antioxidant effects of total flavonoids of Perilla Frutescens leaves in hyperlipidemia rats induced by high-fat diet, Food Res. Int. 44 (1) (2011) 404–409.
[24] Y.C. Li, B.X. Li, L.J. Geng, Hypolipidemic and antioxidant effects of total flavonoids from blueberry leaves, Eur. Food Res. Technol. 233 (2011) 897–903.
[25] Y. He, Y. Shi, A. Zhang, X. Zhang, J. Sun, L. Tian, Lipid-lowering and antioxidative effects of Apium graveolens L. root flavonoid extracts, RSC Adv. 9 (46) (2019) 26757–26767.
[26] T.-I. Jeon, T.F. Osborne, SREBPs: metabolic integrators in physiology and metabolism, Trends Endocrinol. Metabol. 23 (2012) 65–72.
[27] J.D. Horton, J.L. Goldstein, M.S. Brown, SREBPs: activators of the complete program of cholesterol and fatty acid synthesis in the liver, J. Clin. Invest. 109 (2002) 1125–1131.
[28] Q. Hu, Y. Mao, M. Liu, R. Luo, R. Jiang, F. Guo, The active nuclear form of SREBP1 amplifies ER stress and autophagy via regulation of PERK, FEBS J. 287 (2019) 2348–2366.

[29] L. Chen, Y. Duan, H. Wei, H. Ning, C. Bi, Y. Zhao, Y. Qin, Y. Li, Acetyl-CoA carboxylase (ACC) as a therapeutic target for metabolic syndrome and recent developments in ACC1/2 inhibitors, Expet Opin. Invest. Drugs 28 (2019) 917–930.
[30] S. Smith, The animal fatty acid synthase: one gene, one polypeptide, seven enzymes, Faseb. J. 8 (1994) 1248–1259.
[31] M. Karpale, A.J. Käräjämäki, O. Kummu, H. Gylling, T. Hyötyläinen, M. Orešič, A. Tolonen, H. Hautajärvi, M.J. Savolainen, M. Ala-Korpela, J. Hukkanen, J. Hakkola, Activation of pregnane X receptor induces atherogenic lipids and PCSK9 by a SREBP2-mediated mechanism, Br. J. Pharmacol. 178 (12) (2021) 2461–2481.
[32] B.A. Ference, J.G. Robinson, R.D. Brook, A.L. Catapano, M.J. Chapman, D.R. Neff, S. Voros, R.P. Giugliano, G. Davey Smith, S. Fazio, M.S. Sabatine, Variation in PCSK9 and HMGCR and risk of cardiovascular disease and diabetes, N. Engl. J. Med. 375 (2016) 2144–2153.
[33] W.H. Frishman, Can clinicians improve on the effectiveness of statins with additional lipid-lowering therapies? Am. J. Med. 128 (2015) 1160–1161.
[34] M.A. Liuan, Q. Huiling, L.I. Li, G. Deming, miRNA regulate lipid metabolism via PPAR and AMPK/SREBPs signaling pathway, Chem. Life 37 (2017) 1017–1029.
[35] L. Meoli, D. Ben-Zvi, C. Panciotti, S. Kvas, P. Pizarro, R. Munoz, N. Stylopoulos, Intestine-specific overexpression of LDLR enhances cholesterol excretion and induces metabolic changes in male mice, Endocrinology 160 (2019) 744–758.
[36] Y.-X. Wang, W.-J. Kong, Y.-H. Li, S. Tang, Z. Li, Y.-B. Li, Y.-Q. Shan, C.-W. Bi, J.-D. Jiang, D.-Q. Song, Synthesis and structure–activity relationship of berberine analogues in LDLR up-regulation and AMPK activation, Bioorg. Med. Chem. 20 (2012) 6552–6558.
[37] S. Zhong, L. Li, Y.-L. Zhang, L. Zhang, J. Lu, S. Guo, N. Liang, J. Ge, M. Zhu, Y. Tao, Y.-C. Wu, H. Yin, Acetaldehyde dehydrogenase 2 interactions with LDLR and AMPK regulate foam cell formation, J. Clin. Invest. 129 (2018) 252–267.
[38] D. Guo, F. Reinitz, M. Youssef, C. Hong, D. Nathanson, D. Akhavan, D. Kuga, A.N. Amzajerdi, H. Soto, S. Zhu, I. Babic, K. Tanaka, J. Dang, A. Iwanami, B. Gini, J. Dejesus, D.D. Lisiero, T.T. Huang, R.M. Prins, P.Y. Wen, H.I. Robins, M.D. Prados, L.M. Deangelis, I.K. Mellinghoff, M.P. Mehta, C.D. James, A. Chakravarti, T. F. Cloughesy, P. Tontonoz, P.S. Mischel, An LXR agonist promotes glioblastoma cell death through inhibition of an EGFR/AKT/SREBP-1/LDLR-dependent pathway, Cancer Discov. 2 (2011) 190–191.
[39] O. Bogachev, A. Majdalawieh, X. Pan, L. Zhang, H.-S. Ro, Adipocyte enhancer-binding protein 1 (AEBP1) (a novel macrophage proinflammatory mediator) overexpression promotes and ablation attenuates atherosclerosis in ApoE (-/-) and LDLR (-/-) mice, Mol. Med. 17 (2011) 1056–1064.
[40] Y. Sumida, E. Niki, Y. Naito, T. Yoshikawa, Involvement of free radicals and oxidative stress in NAFLD/NASH, Free Radic. Res. 47 (11) (2013) 869–880.